η-pairing superconductivity in the Hubbard chain with pair hopping

George I. Japaridze, Arno P. Kampf, Michael Sekania, P. Kakashvili, Philipp Brune

Angaben zur Veröffentlichung / Publication details:

Japaridze, George I., Arno P. Kampf, Michael Sekania, P. Kakashvili, and Philipp Brune. 2002. "η-pairing superconductivity in the Hubbard chain with pair hopping." *Physical Review B* 65 (1): 014518. https://doi.org/10.1103/PhysRevB.65.014518.

η-pairing superconductivity in the Hubbard chain with pair hopping

G. I. Japaridze,[1,2] A. P. Kampf,[1] M. Sekania,[1,3] P. Kakashvili,[3] and Ph. Brune[1]
[1]*Institut für Physik, Theoretische Physik III, Elektronische Korrelationen und Magnetismus, Universität Augsburg, 86135 Augsburg, Germany*
[2]*Institute of Physics, Georgian Academy of Sciences, Guramishvili Str. 6, 380077, Tbilisi, Georgia*
[3]*Department of Physics, Tbilisi State University, Chavchavadze Ave. 3, 380028, Tbilisi, Georgia*
(Received 26 June 2000; revised manuscript received 29 June 2001; published 13 December 2001)

The ground-state phase diagram of the one-dimensional Hubbard chain with pair-hopping interaction is studied. The analysis of the model is performed using the continuum-limit field theory approach and exact diagonalization studies. At half-filling the phase diagram is shown to consist of two superconducting states with Cooper-pair center-of-mass momentum $Q=0$ (BCS-η_0 phase) and $Q=\pi$ (η_π phase) and four insulating phases corresponding to the Mott antiferromagnet, the Peierls dimerized phase, the charge-density-wave (CDW) insulator, and an unconventional insulating phase characterized by the coexistence of a CDW and a bond-located staggered magnetization. Away from half-filling the phase diagram consists of the superconducting BCS-η_0 and η_π phases and the metallic Luttinger-liquid phase. The BCS-η_0 phase exhibits a smooth crossover from a weak-coupling BCS type to a strong-coupling local-pair regime. The η_π phase shows the properties of the doublon (zero-size Cooper-pair) superconductor with Cooper-pair center-of-mass momentum $Q=\pi$. The transition into the η_π-paired state corresponds to an abrupt change in the ground-state structure. After the transition the conduction band is completely destroyed and a new η_π-pair band, corresponding to the strongly correlated doublon motion, is created.

DOI: 10.1103/PhysRevB.65.014518 PACS number(s): 71.10.Fd, 71.10.Hf, 71.27.+a, 71.30.+h

I. INTRODUCTION

The problem of a crossover from a weak-coupling BCS picture of Cooper-pair formation[1] to a Bose-Einstein (BE) condensation of preformed local pairs has drawn special interest during the last two decades (see for a review Refs. 2–4). Increased renewed interest to this problem mainly comes from experimental observations regarding the unusual properties of high-T_c materials. Particularly important in this respect is the extreme short (of the order of one lattice spacing) coherence length of the pairs in the superconducting state[5] and a pseudogap structure in the normal-state density of states of underdoped cuprates.[6]

Leggett[7] was the first to point out that BCS superconductivity can be continuously connected to BE condensation by increasing the two-particle attraction between electrons from weak to strong coupling. The size of Cooper pairs shrinks continuously until spatially well-separated bosons form, which undergo Bose condensation at a sufficiently low temperature. Nozieres and Schmitt-Rink[8] have extended Leggett's work to lattice electrons and analyzed the crossover between the BCS and BE limits as a function of coupling strength. The attractive ($U<0$) Hubbard model

$$\mathcal{H}=-t\sum_{n,\sigma}(c^{\dagger}_{n,\sigma}c_{n+1,\sigma}+\text{H.c.})+U\sum_{n}\hat{\rho}_{\uparrow}(n)\hat{\rho}_{\downarrow}(n) \quad (1)$$

was usually considered to describe the evolution from the BCS-type pairing to the local pair (composite boson) limit.[9] Here $c^{\dagger}_{n,\sigma}(c_{n,\sigma})$ is the creation (annihilation) operator for an electron with spin σ at site n and $\hat{\rho}_{\sigma}(n)=c^{\dagger}_{n,\sigma}c_{n,\sigma}$.

A rather different realization of local pairing is the η-pairing mechanism of superconductivity introduced by Yang.[10] Yang discovered a class of eigenstates of the Hubbard Hamiltonian which have the property of off-diagonal long-range order (ODLRO),[11] which in turn implies the Meissner effect and flux quantization.[12,13] These eigenstates are constructed in terms of doublon (on-site singlet pair) creation operators. Following Yang's notation we call these η-paired states. One can consider two different realizations of the η-paired state, constructed in terms of zero-size Cooper pairs with *center-of-mass momentum equal to* zero (η_0 pairing) and π (η_π pairing), respectively. Yang also proved that on a hypercubic lattice these states cannot be ground states for the Hubbard model with finite interaction.[10] The η_0 superconductivity is realized in the ground state of the Hubbard model on a cubic lattice only at infinite on-site attraction.[14] In the case of finite U the ground state of the Hubbard model is of the η_0-pairing type on a very particular lattice and in the restricted range of band fillings.[15] Shortly after Yang's paper, several integrable generalizations of the Hubbard model showing a true ODLRO and η_0 superconductivity in the ground state for a finite on-site interaction were proposed.[16]

The η_π superconductivity is realized in the ground state of the Penson-Kolb-Hubbard (PKH) model, i.e., the extended Hubbard model with pair-hopping interaction.[17–19] In one dimension the Hamiltonian of the PKH model reads

$$\mathcal{H}=-t\sum_{n,\sigma}(c^{\dagger}_{n,\sigma}c_{n+1,\sigma}+\text{H.c.})+U\sum_{n}\hat{\rho}_{\uparrow}(n)\hat{\rho}_{\downarrow}(n)+W\sum_{n}(c^{\dagger}_{n,\uparrow}c^{\dagger}_{n,\downarrow}c_{n+1,\downarrow}c_{n+1,\uparrow}+\text{H.c.})+\mu\sum_{n,\sigma}\hat{\rho}_{\sigma}(n). \quad (2)$$

There are N_e particles and N_0 sites, and the band filling $\nu=N_e/2N_0$ is controlled by the chemical potential μ. In the

absence of the W term the Hamiltonian (2) corresponds to the Hubbard model, while in the absence of the U term it reduces to the Penson-Kolb (PK) model.[20]

It is notable that the pair-hopping term and the Hubbard term could be obtained from the same general tight-binding Hamiltonian[21] by focusing on a selected term of the two-particle interaction. The sign of *Coulomb-driven* on-site and pair-hopping interactions is typically repulsive $U,W>0$. However, we will treat the parameters U,W as effective (phenomenological) ones, assuming that they include all possible renormalizations[19] and their values and signs could be arbitrary.

In the ultimate limit of strong pair-hopping interaction $|W|\gg|U|,t$ the PKH model becomes equivalent to the non-interacting spinless fermion (doublon) model or, equivalently, the spin-1/2 XY model:

$$\mathcal{H}=E_0+W\sum_n\ [\eta_0^+(n)\eta_0^-(n+1)+\text{H.c.}]. \tag{3}$$

Here, $E_0=\frac{1}{2}N_0U$ and the pseudospin operators are

$$\eta_0^+(n)=c_{n,\uparrow}^\dagger c_{n,\downarrow}^\dagger,\quad \eta_0^-(n)=c_{n,\downarrow}c_{n,\uparrow},$$
$$\eta_0^z(n)=(c_{n,\uparrow}^\dagger c_{n,\uparrow}+c_{n,\downarrow}^\dagger c_{n,\downarrow}-1)/2. \tag{4}$$

This picture holds true at $W/t\to\infty$ or $-\infty$ due to the $W\to -W$ invariance of the XY model.

The spinless fermion model is superconducting by construction: electrons only appear as singlet pairs on the same site, while the interaction term acts as a hopping term for these pairs. At $W<0$, $|W|\gg U,t$ the η_0-superconducting correlations

$$\langle\eta_0^+(0)\eta_0^-(n)\rangle\simeq n^{-1/2} \tag{5}$$

dominate in the ground state. Using the unitary transformation $c_n\to i^n c_n$, i.e.,

$$\eta_0^+(n)\to(-1)^n\eta_0^+(n)\equiv\eta_\pi^+(n), \tag{6}$$

which changes the sign of the pair-hopping term, one obtains that at $W>0$ the η_π-superconducting correlations

$$\langle\eta_\pi^+(0)\eta_\pi^-(n)\rangle\simeq n^{-1/2} \tag{7}$$

dominate in the ground state.

At $t\neq 0$, $W\to -W$ is not a symmetry of the PKH model. Therefore, the way the system approaches its limiting behavior at $|W|\gg t$, $|U|$ is genuinely different for negative and positive W.

As we show below, in full agreement with previous studies,[22–24,18] at $U,W<0$ the PKH model describes a *continuous evolution* of the usual BCS-type superconducting state at $|U|,|W|\ll t$ into a local-pair η_0-type state at $|W|/t\to\infty$ and/or $|U|/t\to\infty$.

In contrast, the transition into the η_π-paired state takes place at *finite* $W_c(U,t)$ and is of *first order* (level-crossing type). After the transition the contribution of the one-electron hopping term to the ground-state energy almost vanishes and the ground-state energy approaches its limiting value corresponding to the free spinless fermion (doublon) model. This phenomenon we call the *destruction of the single-particle band* and the *creation of a strongly correlated two-particle η_π-pair band*.

The transition into a η_π-paired phase is a typical *finite-bandwidth phenomenon*: at $U=0$, where the transition point is determined by the competition between the single-electron and doublon delocalization energies, the critical value of the pair-hopping $W_c(U=0)\simeq 1.8t$.[18] As we show in this paper the on-site interaction leads to a substantial renormalization of the critical value: $W_c(U)$ is linear in U for $|U|\leqslant t$ while the strong on-site attraction reduces W_c down to values of order $\sim t^2/|U|$. We believe that this transition is generic for models with the pair-hopping interaction and does not depend on the dimensionality of the system.

In the weak-coupling limit $|U|,|W|\ll t$ the ground-state phase diagram of the PKH model is well described within the continuum-limit (infinite bandwidth) approach.[25] However, due to the finite-bandwidth nature of the transition into an η_π-paired phase, a detailed analysis of the transition is out of range of the applicability of the continuum approaches. Since the characteristic length (size of a "Cooper pair") is almost zero in the η_π-paired phase, the nature of the transition can be studied very accurately, using exact Lanczos diagonalization for short chains. These approaches are complementary to each other. In this paper we present results obtained within both approaches. In the forthcoming section we study the ground-state phase diagram of the PKH chain using the bosonization technique. In Sec. III we study the transition into a η_π phase using exact Lanczos diagonalization for chains up to $L=12$ sites. Finally, Sec. IV is devoted to a discussion and to concluding remarks.

II. WEAK-COUPLING PHASE DIAGRAM

In this section we consider the ground-state phase diagram of the PKH model using the continuum-limit bosonization approach. While this procedure has a long history and is reviewed in many places,[26] we briefly sketch the most important points.

Assuming $|U|,|W|\ll t$ we linearize the spectrum in the vicinity of the Fermi points $\pm k_F$ and pass to the continuum limit by the substitution $c_{n,\sigma}\to e^{ik_Fx}\Psi_{R\sigma}(x)+e^{-ik_Fx}\Psi_{L\sigma}(x)$, $x=na_0$, where a_0 is the lattice spacing and $\Psi_{R,L;\sigma}(x)$ are the right and left components of the Fermi field. These fields can be bosonized in a standard way:

$$\Psi_{R,L;\sigma}(x)=\frac{1}{\sqrt{2\pi a_0}}e^{\pm i\sqrt{4\pi}\Phi_{R,L;\sigma}}, \tag{8}$$

where $\Phi_{R(L);\sigma}$ are the right- (left-) moving Bose fields. We define $\Phi_\sigma=\Phi_{R,\sigma}+\Phi_{L,\sigma}$ and introduce linear combinations $\varphi_c=(\Phi_\uparrow+\Phi_\downarrow)/\sqrt{2}$, and $\varphi_s=(\Phi_\uparrow-\Phi_\downarrow)/\sqrt{2}$, to describe the charge and spin degrees of freedom, respectively. Then, after a rescaling of fields and lengths, the bosonized version of the Hamiltonian (2) acquires the following form:

$$\mathcal{H}=\mathcal{H}_c+\mathcal{H}_s, \tag{9}$$

where

$$\mathcal{H}_s = \int dx \left\{ \frac{v_s}{2}[(\partial_x \varphi_s)^2 + (\partial_x \vartheta_s)^2] + \frac{m_s}{2\pi^2 a_0^2} \cos[\sqrt{8\pi K_s}\varphi_s(x)] \right\} \tag{10}$$

describes the spin degrees of freedom.

The charge degrees of freedom for $\nu \neq 1/2$ are described by the free scalar field

$$\mathcal{H}_c = \frac{v_c}{2} \int dx[(\partial_x \varphi_c)^2 + (\partial_x \vartheta_c)^2] \tag{11}$$

and for $\nu = 1/2$ by the quantum sine-Gordon field

$$\mathcal{H}_c = \int dx \left\{ \frac{v_c}{2}[(\partial_x \varphi_c)^2 + \partial_x \vartheta_c)^2] + \frac{m_c}{2\pi^2 a_0^2} \cos[\sqrt{8\pi K_c}\varphi_c(x)] \right\}. \tag{12}$$

Here $\theta_{c,s}(x)$ are the dual counterparts of the fields $\phi_{c,s}(x)$: $\partial_x \theta_{c,s} = \Pi_{c,s}$ where $\Pi_{c,s}$ is the momentum conjugate to the field $\phi_{c,s}$, $v_{c,s} = v_F K_{c,s}^{-1}$ are the velocities of the charge and spin excitations, and

$$K_c - 1 \simeq \frac{U + 2W}{2\pi v_F}, \quad m_c = -\frac{U - 2W}{\pi v_F}, \tag{13}$$

$$K_s - 1 \simeq \frac{U + 2W}{2\pi v_F}, \quad m_s = \frac{U + 2W}{\pi v_F}, \tag{14}$$

$$v_F = 2(t - W/\pi) a_0 \sin(\pi \nu). \tag{15}$$

The mapping of the Hamiltonian (2) into the quantum theory of two independent charge and spin Bose fields allows us to study the ground-state phase diagram of the initial electron system using the far-infrared properties of the bosonic Hamiltonians (10)–(12).

Let us first consider the half-filled band case when both the spin and the charge sectors of the system are governed by the quantum sine-Gordon (SG) fields. Depending on the relation between the bare coupling constants K and m the infrared behavior of the quantum SG field exhibits two different regimes, as follows.[27]

For $|m| \leqslant 2(K-1)$ we are in the weak-coupling regime; the effective mass $M \to 0$. The low-energy (large distance) behavior of the gapless charge (spin) excitations is described by a free scalar field. The corresponding correlations show a power-law decay

$$\langle e^{i\sqrt{2\pi K^*}\varphi(x)} e^{-i\sqrt{2\pi K^*}\varphi(x')} \rangle \sim |x - x'|^{-K^*}, \tag{16}$$

$$\langle e^{i\sqrt{2\pi/K^*}\theta(x)} e^{-i\sqrt{2\pi/K^*}\theta(x')} \rangle \sim |x - x'|^{-1/K^*}, \tag{17}$$

and the only parameter controlling the infrared behavior in the gapless regime is the fixed-point value of the effective coupling constants $K_{c(s)}^*$.

For $|m| > 2(K-1)$ the system scales into a strong-coupling regime: depending on the sign of the bare mass m, the effective mass $M \to \pm\infty$, which signals the crossover into a strong-coupling regime and indicates the dynamical generation of a commensurability gap in the excitation spectrum. The field $\varphi_{c(s)}$ gets ordered with the vacuum expectation values[28]

$$\langle \varphi \rangle = \begin{cases} \sqrt{\dfrac{\pi}{8K}} & (m > 0), \\ 0 & (m < 0). \end{cases} \tag{18}$$

The ordering of these fields determines the symmetry properties of the possible ordered ground states of the fermionic system.

Using Eqs. (13), (14), and (18) one easily finds that there is a gap in the spin excitation spectrum ($M_s \to -\infty$) for $U + 2W < 0$. In this sector the φ_s field gets ordered with vacuum expectation value $\langle \varphi_s \rangle = 0$. In the sector $U + 2W \geqslant 0$ the spin excitations are gapless and the low-energy properties of the spin sector are described by the free Bose field system with the fixed-point value of the parameter $K_s^* = 1$.

At half-filling the charge sector is gapless for $U, W \leqslant 0$ and along the line $U = 2W$ for $U, W > 0$. At $U, W \leqslant 0$ the low-energy properties of the gapless charge sector are described by the free Bose field Hamiltonian (11) with the fixed-point value of the parameter

$$K_c^* \simeq 1 + \sqrt{2UW}/\pi v_F. \tag{19}$$

For $U, W > 0$ the line $U = 2W$ ($m_c = 0$) corresponding to the fixed-point line $m_c = 0, K_c - 1 < 0$. Here the infrared properties of the gapless charge sector are described by the free massless Bose field with the bare value of the Luttinger-liquid parameter K_c. Moreover, the line $U, W > 0, U = 2W$ separates two different insulating (charge gapped) sectors of the phase diagram: for $U > \max\{2W, 0\}$, $m_c < 0$, $M_c \to -\infty$, and therefore the φ_c field gets ordered with vacuum expectation value $\langle \varphi_c \rangle = 0$; for $2W > \max\{U, 0\}$, $m_c > 0$, $M_c \to +\infty$, and therefore the φ_c field gets ordered with vacuum expectation value $\langle \varphi_c \rangle = \sqrt{\pi/8K_c}$.

Away from half-filling the charge sector is gapless and is described by the free massless Bose field (11). The corresponding correlations (16) and (17) show a power-law decay at large distances with critical indices determined by the bare value of the coupling constant K_c. The spin channel remains massive at $U + 2W < 0$ and gapless for $U + 2W \geqslant 0$.

To clarify the symmetry properties of the ground states of the system in different sectors we introduce the following set of order parameters describing the short-wavelength fluctuations of the site-located charge and spin density,

$$\Delta_{CDW}(n)=e^{i2\pi\nu n}\Sigma_\sigma\hat{\rho}_\sigma(n)\rightarrow\begin{cases}\sin[\sqrt{2\pi K_c}\varphi_c(x)]\cos[\sqrt{2\pi K_s}\varphi_s(x)], & \text{at } \nu=1/2,\\ e^{i\sqrt{2\pi K_c}\varphi_c(x)}\cos[\sqrt{2\pi K_s}\varphi_s(x)], & \text{at } \nu\neq 1/2,\end{cases} \tag{20}$$

$$\Delta_{SDW}(n)=e^{i2\pi\nu n}\Sigma_\sigma\sigma\hat{\rho}_\sigma(n)\rightarrow\begin{cases}\cos[\sqrt{2\pi K_c}\varphi_c(x)]\sin[\sqrt{2\pi K_s}\varphi_s(x)], & \text{at } \nu=1/2,\\ e^{i\sqrt{2\pi K_c}\varphi_c(x)}\sin[\sqrt{2\pi K_s}\varphi_s(x)], & \text{at } \nu\neq 1/2,\end{cases} \tag{21}$$

and two superconducting order parameters corresponding to singlet (Δ_{SS}) and triplet (Δ_{TS}) superconductivity:

$$\Delta_{SS}(x)=\Psi^\dagger_{R\uparrow}(x)\Psi^\dagger_{L\downarrow}(x)-\Psi^\dagger_{R\downarrow}(x)\Psi^\dagger_{L\uparrow}(x)\rightarrow\exp\left(i\sqrt{\frac{2\pi}{K_c}}\theta_c(x)\right)\cos[\sqrt{2\pi K_s}\varphi_s(x)], \tag{22}$$

$$\Delta_{TS}(x)=\Psi^\dagger_{R\uparrow}(x)\Psi^\dagger_{L\downarrow}(x)+\Psi^\dagger_{R\downarrow}(x)\Psi^\dagger_{L\uparrow}(x)\rightarrow\exp\left(i\sqrt{\frac{2\pi}{K_c}}\theta_c(x)\right)\sin[\sqrt{2\pi K_s}\varphi_s(x)]. \tag{23}$$

In the particular case of a half-filled band, we consider an additional pair of order parameters, corresponding to the short-wavelength fluctuations of the bond-located charge and spin density:

$$\Delta_{dimer}(n)=(-1)^n\sum_\sigma(c^\dagger_{n,\sigma}c_{n+1,\sigma}+\text{H.c.})\rightarrow\cos[\sqrt{2\pi K_c}\varphi_c(x)]\cos[\sqrt{2\pi K_s}\varphi_s(x)], \tag{24}$$

$$\Delta_{Bd-SDW}(n)=(-1)^n\sum_\sigma\sigma(c^\dagger_{n,\sigma}c_{n+1,\sigma}+\text{H.c.})\rightarrow\sin[\sqrt{2\pi K_c}\varphi_c(x)]\sin[\sqrt{2\pi K_s}\varphi_s(x)], \tag{25}$$

With these results for the excitation spectrum and the behavior of the corresponding fields, Eqs. (16)–(18), we now discuss the *weak-coupling* ground-state phase diagram of the model (2).

A. Half-filled band case

At half-filling the weak-coupling phase diagram of the PKH model consists of the following sectors (see Fig. 1).

A. $U<0$ and $W<0$: $M_s\neq 0$, $\langle\varphi_s\rangle=0$, $M_c=0$, $K_c^*>1$; The singlet superconducting sector

This sector of the coupling constants corresponds to the strong-coupling regime in the spin channel and gapless charge channel. The dynamical generation of a spin gap accompanied by the ordering of the field φ_s with vacuum expectation value $\langle\varphi_s\rangle=0$ leads to a complete suppression of the spin-density-wave (SDW), bond-located SDW (Bd-SDW), and triplet superconductivity (TS) instabilities. The charge-density-wave (CDW), dimer, and singlet superconducting (SS) instabilities survive and show a power-law decay at large distances:

$$\langle\Delta_{CDW}(x)\Delta_{CDW}(x')\rangle\sim\langle\Delta_{dimer}(x)\Delta_{dimer}(x')\rangle\sim|x-x'|^{-K_c^*}, \tag{26}$$

$$\langle\Delta_{SS}(x)\Delta_{SS}(x')\rangle\sim|x-x'|^{-1/K_c^*}, \tag{27}$$

where K_c^* is the fixed-point value of the parameter K_c. For $U,W<0$, $K_c^*>1$ and the SS instability dominates in the ground state.

Note that, at $W=0$ or $U=0$, $K_c^*=1$ and the CDW, Dimer, and SS correlations show an identical power-law decay at large distances. At $W=0$ coexistence of the CDW and superconducting instabilities in the ground state reflects the high $SU(2)\otimes SU(2)$ symmetry of the half-filled Hubbard model.[29] In the case of the Penson-Kolb model ($U=0$), due to the charge-U(1) symmetry of the pair-hopping term, there

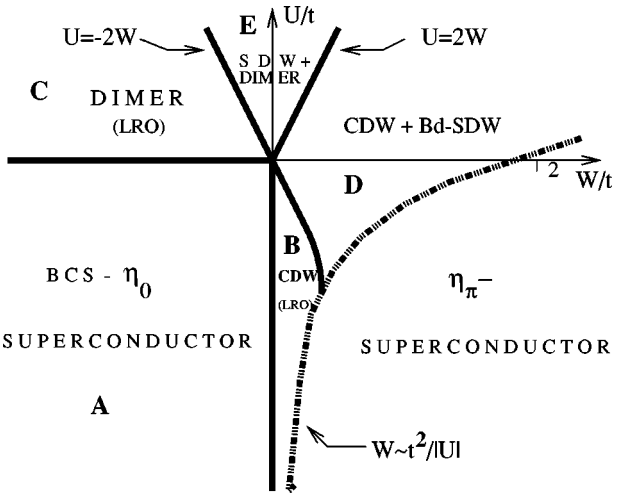

FIG. 1. The ground-state phase diagram of the one-dimensional Penson-Kolb-Hubbard model at half-filling. The dot-dashed line marks a transition into the η_π-superconducting phase. Solid lines separate different phases: A: BCS-η_0-superconductor-singlet superconducting phase exhibiting a continuous evolution with increasing $|U|/t$ and/or $|W|/t$ from the standard BCS limit into the local pair η_0 state. B: CDW (LRO) long-range-ordered (LRO) charge density wave phase. C: Dimer-LRO dimerized (Peierls) phase. D: CDW +Bd-SDW-insulating phase with an identical power-law decay of CDW and bond-located SDW correlations. E: SDW+Dimer-insulating phase with an identical power-law decay of spin-density-wave and Peierls correlations.

is no symmetry reason which guarantees scaling to the SU(2) invariant fixed point $K_c^*=1$. As was shown by Affleck and Marston, the higher-order renormalization group (RG) corrections give $K_c^*>1$, indicating the dominating character of the SS instability in the ground state of the half-filled PK model for arbitrary $W<0$.[22]

B. U<0, 0<W<−U/2: $M_s\neq 0$, $\langle\varphi_s\rangle=0$, $M_c\neq 0$, $\langle\varphi_c\rangle=\sqrt{\pi/8K_c}$; the CDW sector

For $W>0$ the commensurability gap in the charge degrees of freedom opens. For $0<W<-U/2$ the spin sector remains massive. Ordering of the field φ_s with vacuum expectation value $\langle\varphi_s\rangle=0$ leads to a complete supression of the SDW, Bd-SDW, and TS instabilities. Ordering of the field φ_c with vacuum expectation value $\langle\varphi_c\rangle=\sqrt{\pi/8K_c}$ leads to a supression of the SS and dimer correlations. The CDW correlations show a true long-range order,

$$\langle\Delta_{CDW}(x)\Delta_{CDW}(x')\rangle\sim\text{const}, \tag{28}$$

in the ground state. Therefore in this sector of the phase diagram the system displays the properties of the CDW insulator.

C. U>0, 0<U<−2W: $M_s\neq 0$, $\langle\varphi_s\rangle=0$, $M_c\neq 0$, $\langle\varphi_c\rangle=0$; the Peierls (dimerized) sector

Ordering of the field φ_s with vacuum expectation value $\langle\varphi_s\rangle=0$ leads to a complete supression of the SDW, Bd-SDW, and TS instabilities. Ordering of the field φ_c with vacuum expectation value $\langle\varphi_c\rangle=0$ leads to a supression of the SS and CDW correlations. The dimer correlations show a true long-range order,

$$\langle\Delta_{dimer}(x)\Delta_{dimer}(x')\rangle\sim\text{const}, \tag{29}$$

in the ground state. Therefore in this sector of the phase diagram the system is a dimerized (Peierls) insulator.

D. W>0, −2W<U<2W: $M_s=0$, $K_s^*=1$, $M_c\neq 0$, $\langle\varphi_c\rangle=\sqrt{\pi/8K_c}$; the (CDW+Bd-SDW) sector

The generation of a gap in the charge excitation spectrum, accompanied by the ordering of the field φ_c with vacuum expectation value $\langle\varphi_c\rangle=\sqrt{\pi/8K_c}$, leads to a supression of the superconducting, SDW, and dimer ordering. The CDW and Bd-SDW correlations show a power-law decay at large distances:

$$\langle\Delta_{CDW}(x)\Delta_{CDW}(x')\rangle\sim\langle\Delta_{Bd\text{-}SDW}(x)\Delta_{Bd\text{-}SDW}(x')\rangle \sim|x-x'|^{-1}. \tag{30}$$

Therefore this sector of the phase diagram corresponds to the insulating phase with coexisting CDW and Bd-SDW instabilities.

E. U>2|W|: $M_s=0$, $K_s^*=1$, $M_c\neq 0$, $\langle\varphi_c\rangle=0$; the (SDW+dimer) sector

The generation of a gap in the charge excitation spectrum, accompanied by the ordering of the field φ_c with vacuum expectation value $\langle\varphi_c\rangle=0$, leads to a suppression of the superconducting, CDW, and Bd-SDW correlations. The SDW and dimer correlations show a power-law decay at large distances:

$$\langle\Delta_{SDW}(x)\Delta_{SDW}(x')\rangle\sim\langle\Delta_{dimer}(x)\Delta_{dimer}(x')\rangle \sim|x-x'|^{-1}. \tag{31}$$

Therefore this sector of the phase diagram corresponds to the antiferromagnetic insulating phase with coexisting SDW and Peierls instabilities.

B. Non-half-filled band case

Away from half-filling and for $U<0$ the weak-coupling phase diagram of the PKH model consists of the following two sectors.

A1. U+2W<0: $M_s\neq 0$, $\langle\varphi_s\rangle=0$, $M_c=0$, $K_c>1$; the singlet superconducting sector

In this sector of coupling constants the SDW, Bd-SDW, and TS instabilities are suppressed. The CDW, dimer, and SS instabilities show a power-law decay at large distances:

$$\langle\Delta_{CDW}(x)\Delta_{CDW}(x')\rangle\sim\langle\Delta_{dimer}(x)\Delta_{dimer}(x')\rangle \sim|x-x'|^{-K_c}, \tag{32}$$

$$\langle\Delta_{SS}(x)\Delta_{SS}(x')\rangle\sim|x-x'|^{-1/K_c}. \tag{33}$$

For $U=2W<0$, $K_c>1$ and the SS instability dominates in the ground state.

B1. U+2W≥0: $M_s=0$, $K_s^*=1$, $M_c=0$, $K_c<1$; the metallic Luttinger-liquid sector

Both the charge and the spin excitations are gapless. All correlations show a power-law decay in the infrared limit. However, as far as $K_c<1$, the superconducting correlations

$$\langle\Delta_{SS}(x)\Delta_{SS}(x')\rangle\simeq\langle\Delta_{TS}(x)\Delta_{TS}(x')\rangle\sim|x-x'|^{-1-1/K_c} \tag{34}$$

decay faster then the density-density correlations

$$\langle\Delta_i(x)\Delta_i(x')\rangle\sim|x-x'|^{-1-K_c}, \tag{35}$$

where $i\equiv$CDW,SDW,Dimer,Bd-SDW. Therefore in this sector the ground state of the PKH model shows properties of the Luttinger-liquid phase with a weakly dominating tendency towards the density-density-type ordering.

To summarize this section, we have presented the weak-coupling ground-state phase diagram for the one-dimensional (1D) PKH model (see Fig. 2). We have shown that the model has a very rich phase diagram including, at half-filling, the singlet-superconducting phase ($U,W<0$) and four different insulating phases corresponding to the Mott antiferromagnet ($U>2|W|$), the Peierls dimerized insulator ($0<U<-2W$) and the CDW insulator ($W>0,U<-2W$), and an unconventional insulating phase characterized by the coexistence of the CDW and the bond-located staggered magnetization Bd-SDW ($W>0,U<2|W|$). The possibility of bond-located ordering results from the site-off-

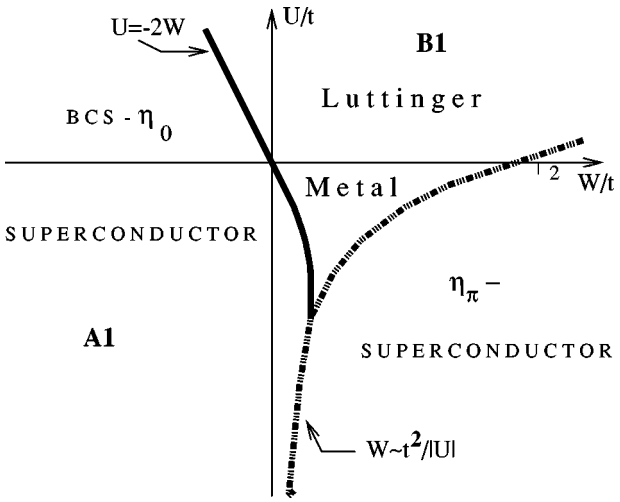

FIG. 2. The ground-state phase diagram of the one-dimensional Penson-Kolb-Hubbard model for $\nu \neq 1/2$. The dot-dashed line marks the transition into the η_π-superconducting phase. The solid line separates the superconducting phase (A1) from the Luttinger metal phase (B1) characterized by an identical power law decay of the SDW, CDW, Bd-SDW, and dimer correlations.

diagonal nature of the pair-hopping term and is a special feature of the half-filled band case.[25] Away from half-filling the phase diagram consists of the singlet-superconducting phase ($U+2W<0$) and the metallic Luttinger-liquid phase ($U+2W>0$).

Note the absence of the η_π-superconducting phase in the weak-coupling phase diagram. This results from the finite-bandwidth nature of this transition. However, the $W \rightarrow -W$ asymmetry of the PKH model as well as the very presence of an additional instability in the system at $W \sim t$ is clearly traced in the additive renormalization of the Fermi velocity (bandwidth) by the pair-hopping term (15). Since the transition into the η_π-paired phase takes place at $W/t \sim 1$, where the continuum-limit RG analysis breaks down, in the forthcoming section we address the study of this transition by using of exact Lanczos diagonalizations for chains up to $L=12$ sites.

III. NUMERICAL STUDIES

In this section using exact diagonalizations studies for chains up to $L=12$ sites we study the transition into the η_π-superconducting phase.

Because the $W \leftrightarrow -W$ asymetry of the phase diagram is connected to two different possibilities for Bose condensation of Cooper pairs with momentum $Q=0$ and $Q=\pi$, it is convenient to rewrite the Hamiltonian (2) in momentum space as

$$\mathcal{H} = -2t \sum_{k,\sigma} c^\dagger_{k,\sigma} c_{k,\sigma} \cos(k) + \sum_Q V(Q) A^\dagger_Q A_Q . \quad (36)$$

Here $V(Q)=U+2W\cos(Q)$ and

$$A^\dagger_Q = \frac{1}{\sqrt{L}} \sum_k c^\dagger_{k,\uparrow} c^\dagger_{Q-k,\downarrow} \quad (37)$$

is the creation operator for a pair of electrons with opposite spins and total momentum Q.

As far as the total momentum of the system Q_{tot} is conserved, one can treat each Q sector of the Hilbert space independently. Since the ground state belongs to the sectors with $Q_{tot}=0$ or $Q_{tot}=\pi$, we restrict ourselves to these sectors only. Let us first consider the simplest case: two particles with opposite spins on the lattice and $U=0$. At $W=0$ the ground-state energy is $E_0=-4t$ and the total momentum is $Q_{tot}=0$. The probability to find an on-site pair in the ground state is $1/L$. Eigenstates in the $Q_{tot}=\pi$ sector correspond to the highly excited states with energy $E=0$. At $|W|/t \rightarrow \infty$ the η_0 pair given by the wave function $A^\dagger_0|0\rangle$ has the energy $E_{\eta_0}=2W$ while the η_π pair given by the wave function $A^\dagger_\pi|0\rangle$ has the energy $E_{\eta_\pi}=-2W$. Therefore, for $W<0$, the ground state *always* remains in $Q_{tot}=0$ subspace and its energy continuously varies from $-4t(W=0)$ to $-2|W|(|W| \gg t)$. The probability to find an on-site pair increases *continuously* up to $1(|W|/t \rightarrow \infty)$. In contrast, for $W>0$, the energy of an η_0-paired state goes to $E_{\eta_0}=2W>0$ while the energy of an η_π-paired state $E_{\eta_\pi}=-2W<0$. Thus, with increasing W/t, at some critical value of the pair-hopping coupling $W_c>0$, the total momentum of the system in the ground state should change from $Q_{tot}=0$ to $Q_{tot}=\pi$. In the $Q_{tot}=\pi$ sector the contribution of the one-particle hopping term to the energy vanishes. Below we will refer to this phenomenon as the *collapse of a one-particle band*. On the other hand, the contribution of the delocalization energy for an η_π pair is equal to $-2W$. Therefore one can roughly estimate the critical value to be $W_c \simeq -2t$.

As we show below, the picture remains qualitatively similar in the case of many-particle systems and $U \neq 0$. The essence of the transition into an η_π-paired state consists of a collapse of the one-particle band and the creation of a strongly correlated two-particle η-pair band.

We start with the W/t dependence of the ground-state energy for different $U \leqslant 0$. In Fig. 3 we have plotted the ground-state energy of the $L=10$ chain at half-filling as a function of W/t, for selected values of U/t. We clearly observe a different behavior of the ground-state energy for $W>0$ and $W<0$. For $W<0$ the ground-state energy continuously approaches the XY model in the limit $|W| \rightarrow \infty$. Using the Jordan-Wigner transformation the ground-state energy of the XY model is easily found as

$$E^{XY}_{g.s.} = -\sum_{k \leqslant k_F} 2|W|\cos(k), \quad (38)$$

which for an infinite system leads to

$$E^{XY}_{g.s.}/N_e = -2|W|/\pi. \quad (39)$$

There is no trace of any additional transition for $W<0$, in agreement with the density-matrix RG (DMRG) results for $U=0$.[23] However, for $W>0$, the ground-state energy shows

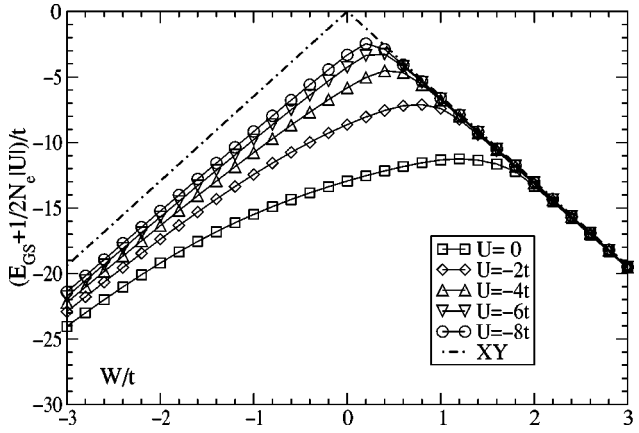

FIG. 3. Ground-state energy of the $L=10$ chain at half-filling, as a function of W/t, for $U/t=0,-2,-4,-6,-8$. The corresponding symbols are indicated in the figure. The dot-dashed line represents the ground-state energy of the pure XY model (38) (i.e., $U=0$) for $L=10$ sites.

a nonmonotonic behavior. We observe that above some critical value of the pair-hopping coupling W_c the energy is already almost linear in W and approaches the ground-state energy of the XY model. Hence for $W>W_c$ the *one-particle hopping term is almost frozen out*. This change of behavior is attributed to the transition to the η_π-superconducting state.[18] An accurate definition for W_c will be given below; however, the numerical data presented in Fig. 3 already clearly indicate the renormalization of the critical value of the pair-hopping coupling W_c by the on-site Hubbard attraction. At $U=0$, $W_c \simeq 1.8t$,[18] and it reduces to $W_c \simeq 0.4t$ at $U/t=-8$.

The critical value of the pair-hopping amplitude corresponding to the transition into an η_π-superconducting state W_c is straightforward to find when the number of electrons is $N_e=2(2n+1)$. The level crossing phenomenon is generic in this case. In Fig. 4(a) we have plotted the lowest-energy levels in each sectors $Q_{tot}=0$ and $Q_{tot}=\pi$ as a function of W/t in the case of a half-filled $L=10$ chain and for $U/t=-4$. Indeed, in this case we observe a well-defined transition from the $Q=0$ to the $Q=\pi$ sector at $W_c=0.625t$. At the same value we observe [see inset in Fig. 4(a)] a singularity in the behavior of the generalized stiffness (GS),

$$\chi(W)=-\partial^2 E_0/\partial W^2|_{U=const},$$

due to the presence of a kink in the ground-state energy $E_0(W)$ at the point where the lowest-energy levels in sectors $Q_{tot}=0$ and $Q_{tot}=\pi$ cross each other. When the number of electrons is $N_e=4n$ the ground state of the system always remains in the sector of momentum space with $Q_{tot}=0$. In Fig. 4(b) we have plotted the ground-state energy of the half-filled PKH model for $L=12$. The insets show the anomaly in the behavior of the generalized stiffness $\chi(W)$ at the same value $W_c=0.625t$ as in the case of $L=10$ chain. This clearly indicates the irrelevance of the finite-size effects already for $L=10$ in the considered case $U/t=-4$. We define the critical value of the pair-hopping amplitude corresponding to the transition into the η_π-paired state at the point where χ exhibits a singularity.

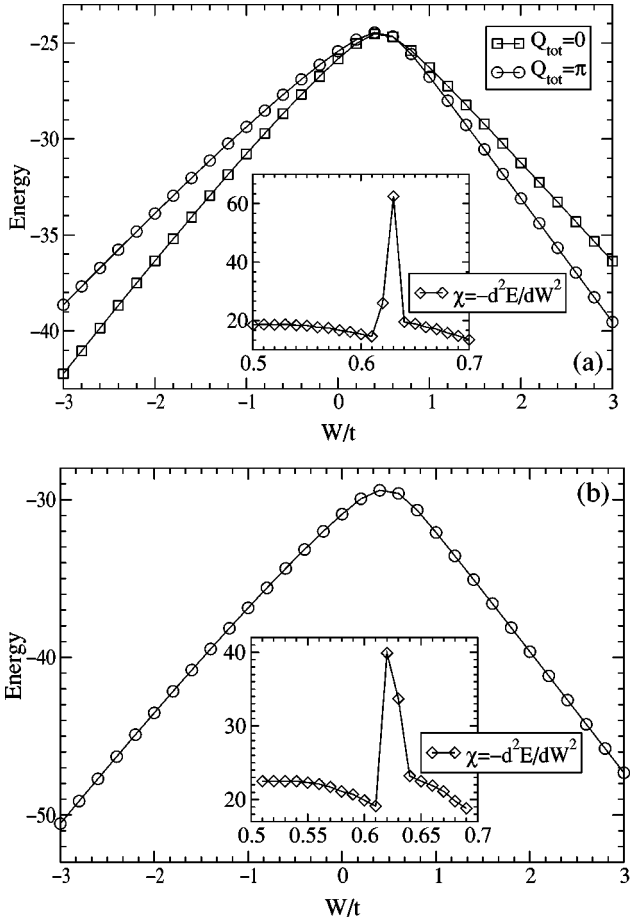

FIG. 4. (a) Lowest energy vs W/t calculated in the $Q_{tot}=0$ (open squares) and $Q_{tot}=\pi$ (open circles) subspaces in the case of a half-filled $L=10$ chain at $U/t=-4$. The inset shows the singularity in the generalized stiffness $\chi(W)=-\partial^2 E_0(W)/\partial W^2$ at $W_c \simeq 0.625t$. (b) Ground-state energy vs W/t for a half-filled $L=12$ chain at $U/t=-4$. The inset in (b) shows the singularity in $\chi(W)$.

Another way to visualize this transition is to show the pairing phenomenon in real space and in momentum space. The corresponding quantities are the expectation values to find an on-site pair,

$$P_{rs}=\frac{1}{L}\sum_{n=1}^{L}\langle \rho_{n\uparrow}\rho_{n\downarrow}\rangle,$$

and the momentum-space pairing probability

$$P_{ms}(Q)=\langle A_Q^\dagger A_Q\rangle.$$

The P_{rs} distribution is shown in Fig. 5. For $W<0$ the pairs appear continuously in the system. In the opposite case $W>0$ and for arbitrary $U<0$, the almost fully paired state is realized in the ground state of the half-filled PKH model for a *finite* value of the pair-hopping amplitude $W>W_c$. However, it should be stressed that due to the quasibosonic character of the pairs, the weight of unpaired particles remains *very small but finite* even for $W \gg W_c$.

In order to clarify the nature of the superconducting phases corresponding to $W>0$ and $W<0$, respectively, we

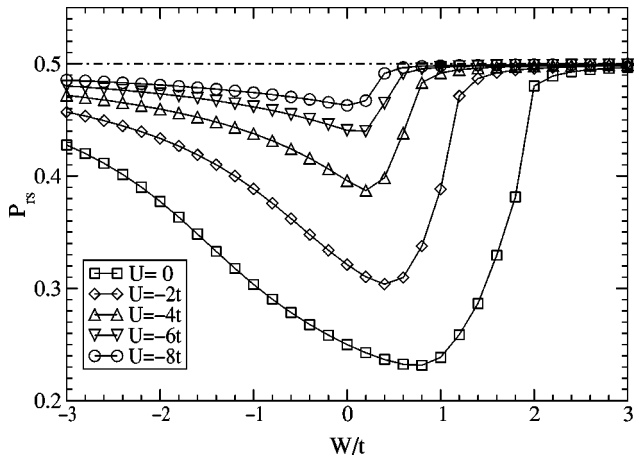

FIG. 5. The real-space pairing probability P_{rs} of the $L=10$ chain at half-filling, as a function of W/t, for $U/t=0,-2,-4,-6,-8$. The corresponding symbols are explained in the figure. The dot-dashed line represents the expectation value to find an on-site pair for the fully paired state $[P_{rs}=N_e/(2L)]$.

show in Fig. 6 the momentum-space pairing probability $P_{ms}(Q)$ as a function of W/t, for $U/t=-4$ for the $L=10$ chain at half-filling. For $W<0$ the distribution $P_{ms}(Q)$ has a peak at $Q=0$. The weight of this peak continuously increases with $|W|/t\to\infty$. The probability to find a π pair is almost zero. At $W>0$, $P_{ms}(Q=0)$ continuously decreases and becomes almost zero at $W>W_c$. However, at $W>W_c$ we observe a drastic change of $P_{ms}(Q)$. The strong peak at $Q=\pi$ appears spontaneously in the distribution $P_{ms}(Q)$. The probability to find a Cooper pair with center-of-mass momentum $Q=\pi$ quickly approaches its limiting value corresponding to the case $W/t=\infty$. The data presented in Fig. 5 and Fig. 6 clearly show the η_π ordering at $W>W_c$.

The transition into the η_π-paired state occurs also away from half-filling. In Fig. 7 we have plotted P_{rs} as a function of W/t for various values of the parameter U/t calculated for the $L=12$ chain and two particular band-fillings $N_e/2L=0.25$ and $N_e/2L=0.33$. As we observe, in contrast to the half-filled case, the transition is now very sharp.

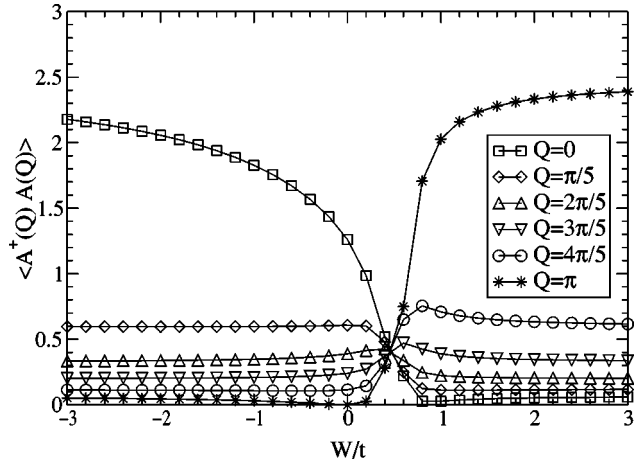

FIG. 6. The distribution $P_{ms}(Q)=\langle A_Q^\dagger A_Q\rangle$ vs W/t for the half-filled PKH chain ($L=10$) at $U=-4t$.

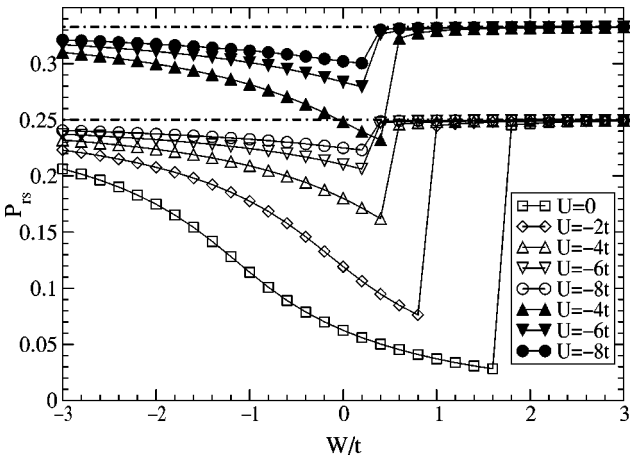

FIG. 7. Real-space pairing probability P_{rs} vs W/t for various values of the parameter U/t for $L=12$, $N_e=8$ (open symbols) and $N_e=6$ (solid symbols). The dot-dashed lines represent the expectation values to find an on-site pair for the fully paired state $[P_{rs}=N_e/(2L)]$.

In order to show the finite-bandwidth nature of the transition into an η_π-superconducting state in Fig. 8 we have plotted the momentum distribution

$$\langle n_k\rangle=\sum_\sigma \langle c_{k\sigma}^\dagger c_{k\sigma}\rangle$$

in the ground state of the $L=10$ half-filled PKH chain as a function of the parameter W/t at $U/t=-4$. In the case of an attractive Hubbard model ($W=0, U=-4t$) the momentum distribution in the ground state has a shape of the standard Fermi distribution: the states with $|k|<k_F=\pi/2$ are almost completely occupied, while the states with $|k|>k_F=\pi/2$ are almost empty. In the case of $W<0$ the momentum distribution remains qualitatively unchanged. With increasing $|W|/t$ the distribution $\langle n_k\rangle$ in a monotonic way approaches its limiting behavior $\langle n_k\rangle=1$ at $|W|/t=\infty$.

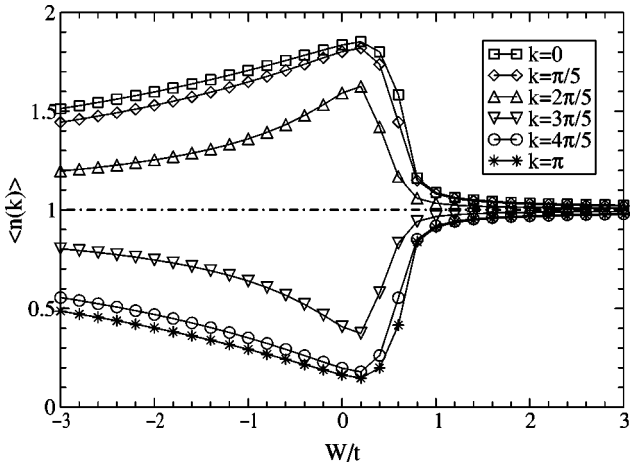

FIG. 8. $\langle n_k\rangle$ distribution for different values of the parameter W/t, in the case of a half-filled $L=10$ chain for $U/t=-4$. The corresponding symbols are explained in the figure.

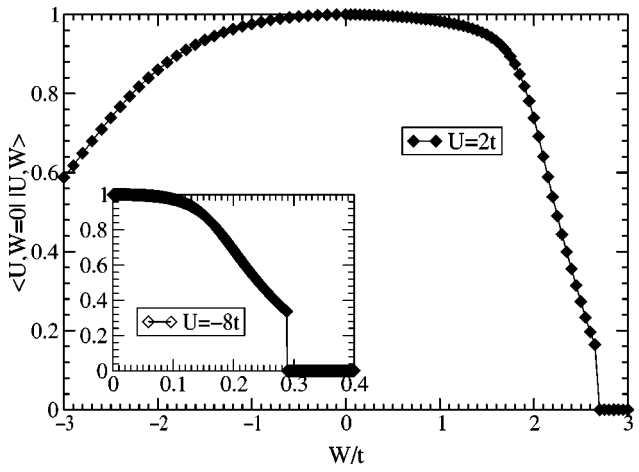

FIG. 9. Overlap integrals of the exact diagonalization ground states of the half-filled ($L=10$) Hubbard model $|U,W=0\rangle$ and the PKH model $|U,W\rangle$ as a function of W and $U=2t$ and $U=-8t$ (inset).

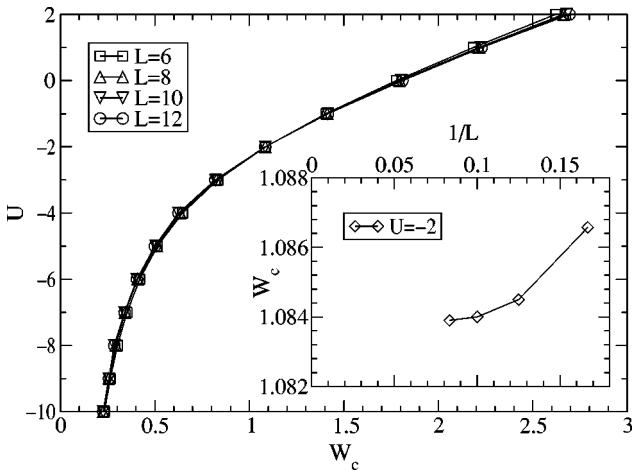

FIG. 10. The phase transition curve into an η_π state for the half-filled PKH chain with $L=6,8,10,12$. The inset in figure shows the finite-size behavior of the parameter W_c at $U=-2t$.

At $W>0$ the standard shape in the momentum distribution remains for $0<W<W_c$; however, at $W\simeq W_c\simeq 0.625t$ we observe an abrupt change in the momentum distribution. For $W>W_c$ $\langle n_k\rangle\simeq 1$ for all k. States with different momenta are almost equally occupied by electrons. There is no trace of the Fermi distribution. As far as states with momentum k and $\pi-k$ are almost equally occupied after the transition, the contribution of the *one-electron band* to the ground-state energy is almost *completely supressed*. The ground-state energy of the system becomes linear in W. Therefore we conclude that the transition into an η_π-superconducting state corresponds to *destruction of the single-electron conduction band* and the *creation of a strongly correlated* η_π*-pair band*.

Figure 9 shows the overlap integrals between the exact ground states of the Hubbard model $|\psi_0^{Hub}\rangle=|U,W=0\rangle$ and of the PKH model $|\psi_0^{PKH}\rangle=|U,W\rangle$ as a function of the pair-hopping coupling for the same values of the Hubbard interaction ($U=2$ and $U=-8$ inset.) The difference from the continuous Kosterlitz-Thouless-type (which is easily studied within the weak-coupling analysis) nature of the transitions into the η_π phase is clearly seen from this data. At $U=2t$ ($U=-8t$) there occurs a transition at $W_c=2.7t$ ($W_c=0.3t$) into a state which is orthogonal to that of the Hubbard model with the same U. In contrast, at $W<W_c$ the ground state changes continuously with W. From this we conclude (in agreement with results of mean-field studies[19]) that the transition into the η_π-superconducting phase is of first order.

Since the transition into an η_π-paired state is connected with the formation of a η_π-pair (doublon) band, after the transition the characteristic length scale in the system $\xi\simeq 0$. Therefore the finite-size effects are very weak. In Fig. 10 we have plotted W_c vs U calculated for the half-filled chain with $L=6,8,10,12$. The inset in Fig. 10 shows the finite-size behavior of the parameter W_c at $U=-2t$. As can be seen in this figure the finite-size effects have only a *very weak* influence on the critical value.

IV. SUMMARY

To summarize, in this paper we have studied the ground-state phase diagram of the one-dimensional Penson-Kolb-Hubbard model using the continuum-limit field theory approach and finite system numerical studies. We have shown that the model has a very rich phase diagram including, at half-filling (see Fig. 1), two different superconducting phases and four different insulating phases corresponding to the singlet-superconducting phase ($U,W<0$) with BCS-type pairing at $|U|,|W|\ll t$, monotonically evolving into the local-pair η_0-superconducting phase with U/t and/or W/t approaching $-\infty$; the η_π-superconducting phase [$W>W_c(U)>0$]; the Mott antiferromagnet ($U>2|W|$) phase, the Peierls dimerized insulator ($0<U<-2W$); the CDW insulator ($W>0, U<-2W$); the unconventional insulating phase characterized with coexistence of the CDW and bond-located staggered magnetization Bd-SDW ($W>0, U<2|W|$).

Away from half-filling (see Fig. 2) the phase diagram consists of the singlet-superconducting phase [$W<\min\{-U/2, W_c(U)\}$], and the metallic Luttinger-liquid (LL) phase [$-U/2<W<W_c(U)$], and the η_π-superconducting phase [$W>W_c(U)>0$]. With increasing on-site attraction the LL phase shrinks, and at a critical value U_c, determined by the condition $U_c+2W_c(U_c)=0$, only the critical line $W_c(U)$ remains for $U<U_c$. In this range of couplings the transition from an η_0 superconductor to an η_π superconductor is realized. The critical value $W_c(U)$ weakly depends on the band-filling ν displaying a nonmonotonic behavior: at $|U|/t\ll 1$ a slight decrease while at $|U|/t\gg 1$ a slight increase with increasing ν.

The obtained phase diagram is in agreement with results of previous studies based on the real-space renormalization group method,[17] the continuum-limit approach,[25] and the slave-boson mean-field method[19] as well as for the particular case of $U=0$ with the results of numerical studies using exact (Lanczos) diagonalizations[18] and DMRG studies.[23]

Using Lanczos diagonalization we have studied in detail the transition into the η_π-paired state. After the transition the

on-site pairing probability sharply approaches its limiting value corresponding to the case $W/t=\infty$ and the η_π-superconducting correlations dominate in the system. The transition corresponds to an abrupt change in the ground-state structure. After the transition the single-electron conduction band is completely destroyed and the strongly correlated η_π-pair (doublon) band is established. The transition occurs at any band filling, the critical value $W_c(U)$ *depends weakly on the band filling* but is strongly renormalized by the on-site Hubbard interaction: $W_c(U)$ is linear in U for $|U|/t$ of the order of unity and is inversely proportional to $|U|$, i.e., $W_c(U)\simeq -t^2/|U|$ for $|U|/t\gg 1$. The DMRG studies of the half-filled PK model ($U=0$) show that the transition into the η_π phase is characterized by closing of a charge gap and opening of a spin gap.[22] We assume that the same behavior is characteristic for the half-filled PKH model for $|U|\sim t$. The detailed studies of the excitation spectrum of the PKH model is under current consideration and will be published elsewhere.

We believe that the above discussed phase diagram is generic for the Penson-Kolb-Hubbard model and will remain unchanged in higher dimensions.

ACKNOWLEDGMENTS

This work was partially supported by the DFG through Grant No. SP 1073. G.J. was partially supported by INTAS-Georgia Grant No. 97-1340. M.S. acknowledges the hospitality at the Institute of Physics, Center for Correlated Electrons and Magnetism of the University of Augsburg, where part of this work was performed.

[1] J. Bardeen, L.N. Cooper, and J.R. Schrieffer, Phys. Rev. **108**, 1175 (1957).

[2] R. Micnas, J. Ranninger, and S. Robaszkiewicz, Rev. Mod. Phys. **62**, 113 (1990).

[3] M. Randeria, in *Bose-Einstein Condensation*, edited by A. Griffin, D. Snoke, and S. Stringari (Cambridge University Press, Cambridge, England, 1995); and in *Models and Phenomenology for Conventional and High-Temperature Superconductivity, Proceedings of the International School of Physics* "*Enrico Fermi*," Course CXXXVI, Varenna, 1997, edited by G. Iadonisi, J.R. Schrieffer, and M.L. Chiofalo (IOS Press, Amsterdam, 1998).

[4] J.M. Singer, T. Schneider, and P.F. Meier, in *Symmetry and Pairing in Superconductors*, edited by M. Ausloos and S. Krichinin (Kluwer Academic, Dordrecht, 1999).

[5] See, for example, *High Temperature Superconductivity*, edited by K. Bedell *et al.* (Addison Wesley, Redwood City, 1990).

[6] H. Ding, T. Yokoya, J.C. Campuzano, T. Takahashi, M. Randeria, M.R. Norman, T. Mochiku, K. Kadowaki, and J. Giapintzakis, Nature (London) **382**, 51 (1996); A.G. Loeser, Z.-X. Shen, D.S. Dessau, D.S. Marshall, C.H. Park, P. Fournier, and A. Kapitulnik, Science **273**, 325 (1996); P. Coleman, Nature (London) **392**, 134 (1998); Ch. Renner, B. Revaz, J.-Y. Genoud, K. Kadowaki, and O. Fisher, Phys. Rev. Lett. **80**, 149 (1998).

[7] A.J. Leggett, J. Phys. (Paris), Colloq. **41**, C7-19 (1980); in *Modern Trends in the Theory of Condensed Matter*, edited by A. Pekalski and J. Przystawa (Springer, Berlin, 1980).

[8] P. Nozieres and S. Schmitt-Rink, J. Low Temp. Phys. **59**, 195 (1985).

[9] S. Robaskiewicz, R. Micnas, and K.A. Chao, Phys. Rev. B **23**, 1447 (1981); R. Frésard, B. Glaser, and P. Wölfle, J. Phys.: Condens. Matter **4**, 8565 (1992); R. Housmann, Z. Phys. B: Condens. Matter **91**, 291 (1993); Phys. Rev. B **49**, 12 975 (1994); M. Randeria, N. Trivedi, A. Moreo, and R.T. Scalettar, Phys. Rev. Lett. **69**, 2001 (1992); N. Trivedi and M. Randeria, *ibid.* **75**, 312 (1995); R.R. dos Santos, Phys. Rev. B **50**, 635 (1994); J.M. Singer, M.H. Pedersen, T. Schneider, H. Beck, and H.-G. Matuttis, *ibid.* **54**, 1286 (1996); M.H. Pedersen, J.J. Rodríguez-Núñez, H. Beck, T. Schneider, and S. Schafroth, Z. Phys. B **103**, 21 (1997); M. Letz and R.J. Gooding, J. Phys.: Condens. Matter **10**, 6931 (1998); M. Keller, W. Metzner, and U. Schollwöck, Phys. Rev. B **60**, 3499 (1999).

[10] C.N. Yang, Phys. Rev. Lett. **63**, 2144 (1989); C.N. Yang and S. Zhang, Mod. Phys. Lett. B **4**, 759 (1990).

[11] C.N. Yang, Rev. Mod. Phys. **34**, 694 (1962).

[12] G.L. Sewell, J. Stat. Phys. **61**, 415 (1995).

[13] H.T. Nieh, G. Su, and B.M. Zhao, Phys. Rev. B **51**, 3760 (1995).

[14] R.R.P. Singh and R.T. Scalettar, Phys. Rev. Lett. **66**, 3203 (1991).

[15] S.-Q. Shen and Z.-M. Qiu, Phys. Rev. Lett. **71**, 4238 (1992); S.-Q. Shen, Int. J. Mod. Phys. B **12**, 709 (1998).

[16] F.H.L. Eßler, V.E. Korepin, and K. Schoutens, Phys. Rev. Lett. **68**, 2960 (1992); *ibid.* **70**, 73 (1993); J. de Boer, V.E. Korepin, and A. Schadschneider, *ibid.* **74**, 789 (1995); J. de Boer and A. Schadschneider, *ibid.* **75**, 4298 (1995); A. Schadschneider, Phys. Rev. B **51**, 10 386 (1995).

[17] B. Bhattacharyya and G.K. Roy, J. Phys.: Condens. Matter **7**, 5537 (1995).

[18] G. Bouzerar and G.I. Japaridze, Z. Phys. B: Condens. Matter **104**, 215 (1997).

[19] S. Robaszkiewicz and B.R. Bułka, Phys. Rev. B **59**, 6430 (1999).

[20] K.A. Penson and M. Kolb, Phys. Rev. B **33**, 1663 (1986); J. Stat. Phys. **44**, 129 (1986).

[21] J. Hubbard, Proc. R. Soc. London, Ser. A **276**, 238 (1963).

[22] I. Affleck and J.B. Marston, J. Phys. C **21**, 2511 (1988).

[23] A.E. Sikkema and I. Affleck, Phys. Rev. B **52**, 10 207 (1995).

[24] M. van den Bossche and M. Caffarel, Phys. Rev. B **54**, 17 414 (1996).

[25] G.I. Japaridze and E. Müller-Hartmann, J. Phys.: Condens. Matter **9**, 10 509 (1997).

[26] See A.O. Gogolin, A.A. Nersesyan, and A.M. Tsvelik, *Bosonization and Strongly Correlated Systems* (Cambridge University Press, Cambridge, England, 1998).

[27] P. Wiegmann, J. Phys. C **11**, 1583 (1978).

[28] K.A. Muttalib and V.J. Emery, Phys. Rev. Lett. **57**, 1370 (1986); T. Giamarchi and H.J. Schulz, Phys. Rev. B **33**, 2066 (1988).

[29] H. Frahm and V.E. Korepin, Phys. Rev. B **42**, 10 553 (1990); N. Kawakami and S.-K. Yang, Phys. Lett. A **148**, 359 (1990).